Physica A 285 (2000) 147–155
PHYSICA A
www.elsevier.com/locate/physa

Periodic solutions of a non-linear traffic model

L.A. Safonov[a,b], E. Tomer[a,*], V.V. Strygin[b], S. Havlin[a]
[a] Department of Physics, Bar-Ilan University, Ramat-Gan, 52900, Israel
[b] Department of Applied Mathematics and Mechanics, Voronezh State University, Voronezh, 394693, Russia

Abstract

A car-following model of single-lane traffic is studied. Traffic flow is modeled by a system of Newton-type ordinary differential equations. Different solutions (equilibria and limit cycles) of this system correspond to different phases of traffic. Limit cycles appear as results of Hopf bifurcations (with density as a parameter) and are found analytically in small neighborhoods of bifurcation points. A study of the development of limit cycles with an aid of numerical methods is performed. The experimental finding of the presence of a two-dimensional region in the density-flux plane is explained by the finding that each of the cycles has its own branch of the fundamental diagram.

Keywords: Cellular automata; Complex systems; Traffic flow

1. Introduction

Traffic flow has been a subject of intensive research in recent decades [1–25]. Special attention has been paid recently to the problem of classification of different phases of traffic based on experimental measurements [7–11] and modeling (e.g. [12–15]).

Kerner and Rehborn [7,8] found experimentally the existence of three phases in traffic: free flow (observed for low values of density, all cars move without hindrance with the preferred velocity and the flux grows with the density), traffic jams (for high values of density, cars move slowly and the flux decreases as density increases) and synchronized flow (for intermediate values of density). The latter phase is characterized by weak correlations between flux and density. Neubert et al. [9] distinguished between synchronized flow and stop-and-go traffic states in the intermediate range of densities. Stop-and-go traffic is characterized by a strong correlation (or anticorrelation)

* Corresponding author. Fax: +972-3-535-3298.
E-mail address: tomer@alon.cc.biu.ac.il (E. Tomer).

0378-4371/00/$ - see front matter
PII: S0378-4371(00)00278-8

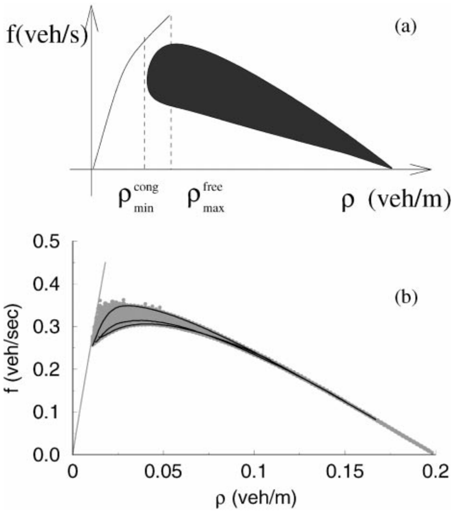

Fig. 1. (a) Dependence of the flux f on the density ρ (schematic) as reported in [11]. (b) Density-flux relation for stable states of the model, obtained by simulations of the model starting with different (homogeneous, random and harmonic) initial conditions, after a long transient time (grey). Each of the three black curves corresponds to the density-flux relation for a certain "wavelength" (in terms of number of cars).

between flux and density as well as periodicity in time [9] and space [10]. According to experimental observations [10,11], different values of flux in synchronized flow may correspond to the same value of density and vice versa. In other words, the dependence of the flux f on the density ρ has the form schematically shown in Fig. 1a.

The existence of a two-dimensional region in the density-flux plane has not been explained by models [11]. A recent car-following model [12] demonstrates the existence of this phenomenon. In the deterministic version of this single-lane car-following model the motion of each car is described by a Newton-type second-order differential equation. The acceleration of a car is assumed to depend on its distance to the car ahead, its velocity, and the difference in velocities between successive cars. A permitted velocity is considered and closed boundary conditions are applied.

Assuming that the number of cars in the system is N, the traffic flow in the model is described by a system of $2N$ first-order differential equations. In [12] it was shown that different phases in real traffic are associated with different solutions of this system. For example, free and jammed flow phases correspond to an equilibrium and the synchronized flow phase is associated with limit cycles. Such an analogy has been established before in other models (e.g. [15]) which use the dynamical system approach to traffic modeling. But to the best of our knowledge none of those models has reported the presence of more than one such cycle.

An important result in Ref. [12] is the presence of *many* limit cycles in the dynamical system, mentioned above. It is suggested that each of these cycles has its own branch of fundamental diagram and all these branches lie inside the two-dimensional region

(Fig. 1b). Thus, the introduced model apart from demonstrating many experimentally observed features of traffic flow also provides an explanation of this phenomenon unexplained before.

In the present paper a detailed analysis of the above-mentioned periodic solutions is given. A combination of analytical and numerical tools is used. It is found that as ρ changes bifurcations of small cycles from an equilibrium occur in the system. For values of density close to bifurcation points these cycles are found approximately using the approach described in Section 3. For other density values numerical procedures are used to find the cycles (Section 4).

2. The model

The model presented in Ref. [12] (in the deterministic case) assumes that the nth car acceleration is

$$a_n = A\left(1 - \frac{\Delta x_n^0}{\Delta x_n}\right) - \frac{Z^2(-\Delta v_n)}{2(\Delta x_n - D)} - kZ(v_n - v_{\mathrm{per}})\,,$$

where x_n is the car's coordinate, v_n its velocity, A the sensitivity parameter, D the minimal distance between consecutive cars, v_{per} the permitted velocity, k a constant parameter, T the safety time gap and $\Delta x_n^0 = v_n T + D$ the safety distance. The function Z is defined as $Z(x) = (x + |x|)/2$.

Therefore, the motion of cars is described by the following system of $2N$ nonlinear ordinary differential equations

$$\dot{x}_n = v_n\,,$$

$$\dot{v}_n = A\left(1 - \frac{v_n T + D}{x_{n+1} - x_n}\right) - \frac{Z^2(v_n - v_{n+1})}{2(x_{n+1} - x_n - D)} - kZ(v_n - v_{\mathrm{per}})\,, \tag{1}$$

$n = 1,\dots,N$ with periodic boundary conditions $x_{N+1} = x_1 + N/\rho$, $v_{N+1} = v_1$.

System (1) has a solution

$$v_n^0 = v^0 = \begin{cases} \dfrac{A(1 - D\rho) + kv_{\mathrm{per}}}{A\rho T + k}, & \rho \leqslant \dfrac{1}{D + Tv_{\mathrm{per}}}, \\[2ex] \dfrac{1 - D\rho}{\rho T}, & \rho \geqslant \dfrac{1}{D + Tv_{\mathrm{per}}}, \end{cases} \qquad x_n^0 = \frac{n-1}{\rho} + v^0 t\,, \tag{2}$$

$(n = 1,\dots,N)$, which corresponds to homogeneous flow.

It is easy to verify that (1) in variables $\{\delta_n = x_{n+1} - x_n\}$, v_n has an equilibrium solution $\delta_1 = \cdots = \delta_N = 1/\rho$, $v_1 = \cdots = v_N = v_0$.

The linearization of Eq. (1) near this equilibrium has the form

$$\ddot{\xi}_n = -p\dot{\xi}_n + q(\xi_{n+1} - \xi_n), \quad n = 1,\dots,N\,, \tag{3}$$

where $\xi_n = \delta_n - 1/\rho$ $(n = 1,\dots,N)$, $\xi_{N+1} = \xi_1$,

$$p = AT\rho + k,\ q = \frac{AT + kTv_{\mathrm{per}} + kD}{AT\rho + k} \cdot A\rho^2 \quad \text{if } \rho \leqslant \frac{1}{D + Tv_{\mathrm{per}}}\,,$$

$$p = AT\rho,\ q = A\rho \qquad\qquad \text{otherwise}\,.$$

Similar to [16,17], a solution of Eq. (3) can be written as

$$\xi_n = \exp\{\mathrm{i}\alpha_\kappa n + zt\}\,, \tag{4}$$

where $\alpha_\kappa = (2\pi/N)\kappa$ $(\kappa = 0,\dots,N-1)$ and z is a complex number. Substituting (4) into (3) we obtain the algebraic equation for z

$$z^2 + pz - q(\mathrm{e}^{\mathrm{i}\alpha_\kappa} - 1) = 0\,. \tag{5}$$

Each of the N equations (5) has two solutions. These $2N$ complex numbers are the eigenvalues of system (3). For $\rho < 1/(D + Tv_{\mathrm{per}})$ and $\rho > 2/AT^2$ all but one (which is zero) of them are negative which indicates the stability of the homogeneous flow solution. As ρ decreases pairs of complex conjugate eigenvalues may cross the imaginary axis which causes the formation of small periodic solutions (Hopf bifurcations).

The next section is devoted to the approximate finding of these periodic solutions for ρ in the vicinities of their bifurcation points.

3. Study of bifurcations of small periodic solutions

For the study of bifurcations, we propose the following common approach. Let (1) be written as

$$\dot{x} = f(x, \rho)\,, \tag{6}$$

where $x = (\xi_1, w_1, \xi_2, w_2, \dots, \xi_N, w_N)^{\mathrm{T}} \in \mathbf{R}^{\mathbf{2N}}$ and $w_n = v_n - v_0$. The homogeneous flow solution (2) corresponds to the zero solution of (6).

For future steps we need system (6) written as

$$\dot{x} = M(\rho)x + f_2(x, \rho) + \mathcal{R}(x, \rho)\,, \tag{7}$$

where

$$M(\rho) = \begin{pmatrix} 0 & -1 & 0 & 1 & 0 & \dots & 0 & 0 \\ q & -p & 0 & 0 & 0 & \dots & 0 & 0 \\ 0 & 0 & 0 & -1 & 0 & \dots & 0 & 0 \\ 0 & 0 & q & -p & 0 & \dots & 0 & 0 \\ \cdot & \cdot & \cdot & \cdot & \cdot & \cdot & \cdot & \cdot \\ 0 & 1 & 0 & 0 & 0 & \dots & 0 & -1 \\ 0 & 0 & 0 & 0 & 0 & \dots & q & -p \end{pmatrix}$$

is the linearization of (6) near zero, $f_2(x,\rho)$ are the second-order terms and $\mathscr{R}(x,\rho)$ are the higher-order terms.

Let for $\rho=\rho_0$ the matrix $M_0=M(\rho_0)$ have a pair of imaginary eigenvalues $\pm\,\mathrm{i}\omega$. The bifurcation problem is closely connected with $2\pi/\omega$-periodic solutions of systems

$$\dot{x}=M_0x \tag{8}$$

and

$$\dot{x}=-M_0^Tx\,. \tag{9}$$

We can find $2\pi/\omega$-periodic solutions $\varphi_1(t)$, $\varphi_2(t)$ of (8) and $\psi_1(t)$, $\psi_2(t)$ of (9) such that

$$\frac{\omega}{2\pi}\int_0^{2\pi/\omega}\langle\varphi_i(t),\psi_j(t)\rangle\,\mathrm{d}t=\delta_{ij}\,, \tag{10}$$

where $i,j=1,2$ and δ_{ij} is the Kronecker symbol.

Note, that if λ is an eigenvalue of matrix M_0, the corresponding eigenvector can be found as

$$h(\lambda)=\left(\mathrm{e}^{\mathrm{i}\alpha_\kappa},\frac{q\mathrm{e}^{\mathrm{i}\alpha_\kappa}}{\lambda+p},\mathrm{e}^{2\mathrm{i}\alpha_\kappa},\frac{q\mathrm{e}^{2\mathrm{i}\alpha_\kappa}}{\lambda+p},\ldots,\mathrm{e}^{(N-1)i\alpha_\kappa},\frac{q\mathrm{e}^{(N-1)i\alpha_\kappa}}{\lambda+p},1,\frac{q}{\lambda+p}\right)^T\,,$$

since λ is a solution of (5) for some κ.

An eigenvector of $-M_0^T$ corresponding to λ can be found similarly. Therefore, we can find $\varphi_1(t)=\cos\omega t\,\mathrm{Re}\,h(\mathrm{i}\omega)-\sin\omega t\,\mathrm{Im}\,h(\mathrm{i}\omega)$ and $\varphi_2(t)=\cos\omega t\,\mathrm{Im}\,h(\mathrm{i}\omega)+\sin\omega t\,\mathrm{Re}\,h(\mathrm{i}\omega)$. Functions $\psi_1(t)$ and $\psi_2(t)$ can be found in the same manner using the eigenvectors of $-M_0^T$ corresponding to $\mathrm{i}\omega$ and then orthogonalized to fit (10).

Let $\rho=\rho_0+\varepsilon$. Then $M(\rho)=M(\rho_0+\varepsilon)=M_0+\varepsilon B+O(\varepsilon^2)$, where $B=\partial M(\rho_0)/\partial\rho$ and system (7) can be rewritten as

$$\dot{x}=M_0(\rho)x+\varepsilon Bx+f_2(x,\rho_0+\varepsilon)+O[(||x||+|\varepsilon|)^3]\,. \tag{11}$$

In order to find a small cycle we introduce a new parameter c, such that [26]

$$\varepsilon=c\gamma_1+c^2\gamma_2+\cdots \tag{12}$$

and the new time

$$\tau=\frac{t}{1+h_1c+h_2c^2+\cdots}\,, \tag{13}$$

where $h_1,h_2,\ldots$ and $\gamma_1,\gamma_2,\ldots$ are yet unknown parameters. We are looking for a small cycle in the form

$$x(\tau)=cx_1(\tau)+c^2x_2(\tau)+\cdots\,,$$

where x_1, $x_2,\ldots$ are unknown functions of τ.

Substituting (12) and (13) into (11) and equating the terms of the same powers of ε, we obtain that $x_1(\tau)$ is a $2\pi/\omega$-periodic solution of (8). We can assign $x_1(\tau) \equiv \varphi_1(\tau)$.

$x_2(\tau)$ can be found as a $2\pi/\omega$-periodic solution of

$$\frac{\mathrm{d}x_2}{\mathrm{d}\tau} = M_0 x_2 + \mathscr{F}_2(\varphi_1(\tau), h_1, \gamma_1)\,, \tag{14}$$

where

$$\mathscr{F}_2(\varphi_1(\tau), h_1, \gamma_1) = -h_1 M_0 \varphi_1(\tau) + \gamma_1 B \varphi_1(\tau) + f_2(\varphi_1(\tau), \rho_0)\,.$$

As shown in [27], for system (14) to have a periodic solution it is necessary and sufficient that

$$\int_0^{2\pi/\omega} \langle \mathscr{F}_2(\varphi_1(\tau), h_1, \gamma_1), \psi_i(\tau)\rangle \,\mathrm{d}\tau = 0\,,$$

for $i = 1, 2$. This condition yields two equations with unknown h_1 and γ_1. Therefore, the periodic solution of (11) can be approximately found as

$$x^*(t) = \frac{\varepsilon}{\gamma_1}\varphi_1(t)\,. \tag{15}$$

This solution has the period $T = (2\pi/\omega)(1 + h_1\varepsilon/\gamma_1) + O(\varepsilon^2)$. Higher approximations of the solution can be found using the algorithm described above. Note that according to (4) there is an integer $1 \leqslant \kappa \leqslant N - 1$ such that the flow state corresponding to solution (15) is a wave with the wavelength L/κ (in length units) or N/κ (in number of cars). In the following, we shall call this solution "κ-cycle".

4. Numerical study of periodic solutions

Each of the small cycles found using the approach proposed in the previous section can be used as initial data for numerical analysis of periodic (in variables ξ_n, w_n) solutions of (1) for density values far from the bifurcation points. Fig. 2 demonstrates the development of these periodic solutions as ρ decreases. Computations are performed so that ρ is changed by a small value and the results of computations from the previous step are taken as initial data. In total, nine bifurcations were detected in this simulation ($\kappa = 1, \ldots, 9$), but all the cycles except for 5-, 6-, 7- and 8-cycles lost stability at high-density values as illustrated in Fig. 2b. Note that the above-mentioned four cycles remain stable even for $\rho < 1/(D + Tv_{\mathrm{per}}) = 0.01818\ldots$, which supports the well-known experimental finding of the coexistence of free and congested traffic regimes in a range of densities.

Fig. 3 illustrates the development of the solutions shown in Fig. 2 (5-, 6-, 7- and 8-cycles top to bottom). The graphs on the left-hand side present the distribution of ξ_n and v_n for different values of ρ. The bifurcation density value ρ_0 and κ corresponding

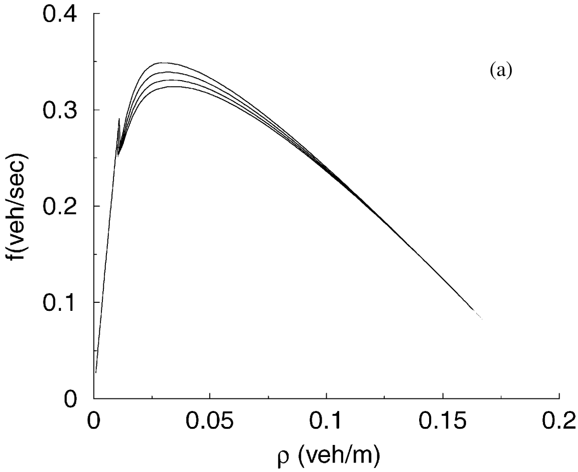

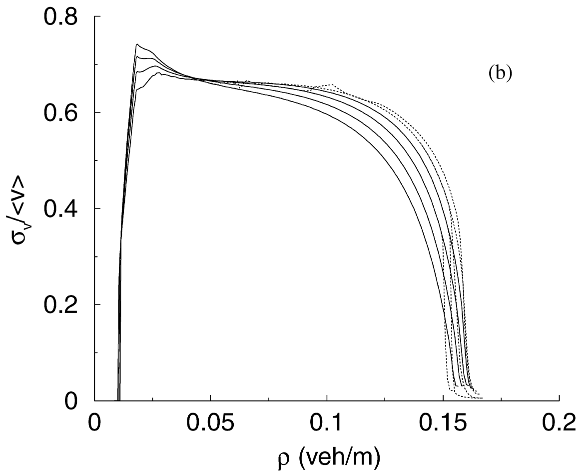

Fig. 2. (a) Fundamental diagrams of four different periodic solutions (5-, 6-, 7- and 8-cycles, top to bottom) for $N = 100$, $A = 3$ m/s^2, $k = 2$ s^{-1}, $v_{\rm per} = 25$ m/s, $D = 5$ m. A straight line for low density values corresponds to the homogeneous flow solution. (b) Dependence of mean-square variation of velocities σ_v (divided by the average over the velocities of all cars $\langle v \rangle$) on ρ. Solid lines correspond to the four cycles shown in (a), dotted lines correspond to other cycles which lost stability at high values of density.

to each solution is specified. The smallest loop on each graph is the solution found analytically for ρ close to ρ_0 using the approach presented in Section 3. The other loops represent the same solutions found numerically with decreasing ρ by steps of $\Delta\rho = 0.01$. The right-hand-side graphs show the dependence of ξ_n on n for corresponding periodic solutions. The sinusoidal plot with smaller amplitude corresponds to the smallest loop in the left-hand-side plot and the other plot to the fourth loop from inside.

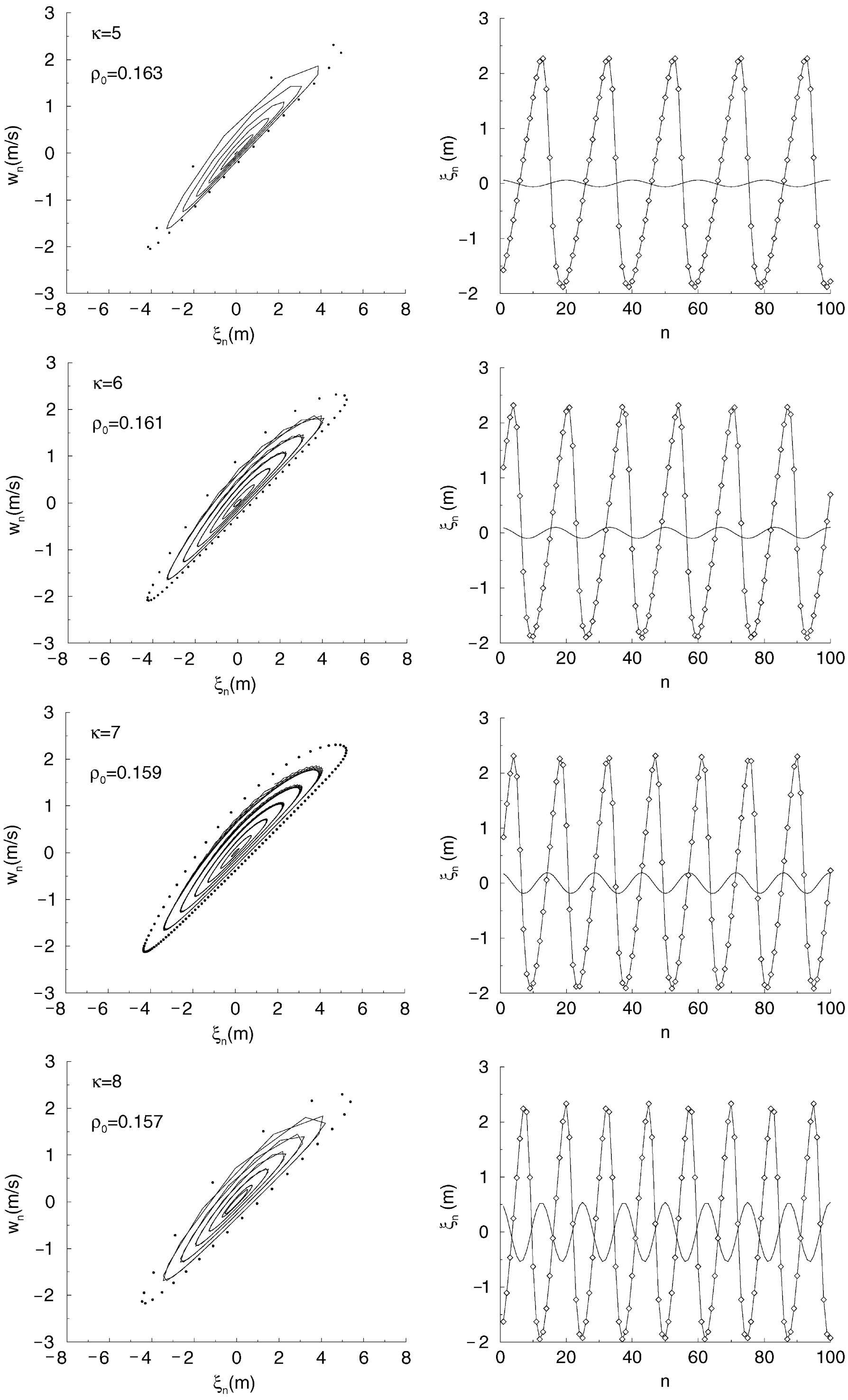

Fig. 3. Development of the four different periodic solutions (Fig. 2a) for decreasing ρ.

Conclusion

We studied a model of single-lane traffic flow, which is described by a system of non-linear ordinary differential equations. The occurrence of inhomogeneities in congested traffic is related to Hopf bifurcations in this system. Density values for which new cycles emerge are found and the cycles themselves are derived analytically near bifurcation points. The dynamics of these cycles far from bifurcation points is studied using numerical methods. It is found that each of these cycles has its own branch of fundamental diagram which suggests an explanation to the experimental finding of the presence of a two-dimensional region in the density-flux plane.

References

[1] M.J. Lighthill, G.B. Whitham, Proc. R. Soc. London Ser. A 229 (1955) 281.
[2] I. Prigogine, Kinetic Theory of Vehicular Traffic, American Elsevier, New York, 1971.
[3] A.D. May, Traffic Flow Foundations, Prentice-Hall, Englewood Cliffs, NJ, 1990.
[4] K. Nagel, M. Schreckenberg, J. Phys. I (France) 2 (1992) 2221.
[5] D.E. Wolf, M. Schreckenberg, A. Bachem (Eds.), Proceedings of Workshop on Traffic and Granular Flow (1995, Julich), World Scientific, Singapore, 1996.
[6] M. Schreckenberg, D.E. Wolf (Eds.), Proceedings of Workshop on Traffic and Granular Flow (1997, Duisburg), Springer, Singapore, 1998.
[7] B.S. Kerner, H. Rehborn, Phys. Rev. E 53 (1996) R4275.
[8] B.S. Kerner, H. Rehborn, Phys. Rev. Lett. 79 (1997) 4030.
[9] L. Neubert, L. Santen, A. Schadschneider, M. Schreckenberg, Phys. Rev. E 60 (1999) 6480.
[10] B.S. Kerner, Phys. Rev. Lett. 81 (1998) 3797.
[11] B.S. Kerner, Physics World 12 (8) (1999) 25.
[12] E. Tomer, L. Safonov, S. Havlin, Phys. Rev. Lett. 84 (2000) 382.
[13] D. Helbing, A. Hennecke, M. Treiber, Phys. Rev. Lett. 82 (1999) 4360.
[14] D. Helbing, M. Treiber, Science 282 (1998) 2001.
[15] H.Y. Lee, H.-W. Lee, D. Kim, Phys. Rev. Lett. 81 (1998) 1130.
[16] M. Bando, K. Hasebe, A. Nakayama, A. Shibata, Y. Sugiyama, Phys. Rev. E 51 (1995) 1035.
[17] Y. Sugiyama, in: D.E. Wolf, M. Schreckenberg, A. Bachem (Eds.), Proceedings of Workshop on Traffic and Granular Flow (1995, Julich), World Scientific, Singapore, 1996, p. 137.
[18] O. Biham, A.A. Middleton, D. Levine, Phys. Rev. A 46 (1992) R6124.
[19] K. Nagel, Phys. Rev. E 53 (1996) 4655.
[20] D.E. Wolf, Physica A 263 (1999) 438.
[21] D. Helbing, M. Schreckenberg, Phys. Rev. E 59 (1999) R2505.
[22] S. Cheybani, J. Kertesz, M. Schreckenberg, J. Phys. A 31 (1998) 9787.
[23] D. Chowdhury, L. Santen, A. Schadschneider, Phys. Rep. 329 (2000) 199.
[24] M. Fukui, Y. Ishibashi, J. Phys. Soc. Jap. 66 (1997) 385.
[25] K. Nagel, H. Herrmann, Physica A 199 (1993) 254.
[26] E.Ya. Zhuravleva, V.V. Strygin, Prikladnaya Matematika i Mekhanika 39 (1975) 369 (in Russian).
[27] I.G. Malkin, Some problems of theory of nonlinear oscilations, U.S. Atomic Energy Commission, Washington, DC, 1959.